The impact of snow depth, snow density and ice density on sea ice thickness retrieval from satellite radar altimetry: Results from the ESA-CCI Sea Ice ECV Project Round Robin Exercise

S. Kern[1], K. Khvorostovsky[2], H. Skourup[3], E. Rinne[4], Z. S. Parsakhoo[1,*], V. Djepa[5], P. Wadhams[5], and S. Sandven[2]

[1]{Center for Climate System Analysis and Prediction CliSAP, University of Hamburg, Hamburg, Germany}

[2]{Nansen Environmental and Remote Sensing Center NSERC, Bergen, Norvay}

[3]{Danish Technical University-Space, Copenhagen, Denmark}

[4]{Finnish Meteorological Institute FMI, Helsinki, Finland}

[5]{University of Cambridge, Cambridge, UK}

[*]{now at: Institute for Meteorology and Geophysics, University of Köln, Köln, Germany}

Correspondence to: S. Kern (stefan.kern@zmaw.de)

Abstract

One goal of the European Space Agency Climate Change Initiative sea ice Essential Climate Variable project is to provide a quality controlled 20-year long data set of Arctic Ocean winter-time sea ice thickness distribution based on satellite radar altimetry. An important step to achieve this goal is to assess the usefulness of assumptions and input parameters used for freeboard-to-thickness conversion. For this purpose a data base is created comprising sea ice freeboard derived from satellite radar altimetry between 1993 and 2012 and collocated observations of total (sea ice + snow) and sea ice freeboard from Operation Ice Bridge (OIB) and CryoSat Validation Experiment (CryoVEx) air-borne campaigns, of sea ice draft from moored and submarine Upward Looking Sonar (ULS), and of snow depth from OIB

campaigns, Advanced Microwave Scanning Radiometer aboard EOS (AMSR-E) and the Warren Climatology (Warren et al., 1999). An inter-comparison of the snow depth data sets stresses the limited usefulness of Warren climatology snow depth for freeboard-to-thickness conversion under current Arctic Ocean conditions reported in other studies. This is confirmed by a comparison of snow freeboard measured during OIB and CryoVEx and snow freeboard computed from radar altimetry. For first-year ice the agreement between OIB and AMSR-E snow depth within 0.02 m suggests AMSR-E snow depth as an appropriate alternative. Different freeboard-to-thickness and freeboard-to-draft conversion approaches are realized. The mean observed ULS sea ice draft agrees with the mean sea ice draft computed from radar altimetry within the uncertainty bounds of the data sets involved. However, none of the realized approaches is able to reproduce the seasonal cycle in sea ice draft observed by moored ULS satisfactorily. A sensitivity analysis of the freeboard-to-thickness conversion suggests: in order to obtain sea ice thickness as accurate as 0.5 m from radar altimetry, besides a freeboard estimate with centimetre accuracy, an ice-type dependent sea ice density is as mandatory as a snow depth with centimetre accuracy.

1 Introduction

As part of the European Space Agency (ESA) Climate Change Initiative (CCI) sea ice Essential Climate Variable (ECV) project (SICCI project) quality-controlled long-term data sets of sea ice thickness and concentration will be derived from Earth observation data. The product of sea ice thickness and sea ice area is the sea ice volume which is considered to be among the most sensitive indicators of the amplification of Climate change in the Arctic (Schweiger et al., 2011; Zhang et al., 2012; Krinner et al., 2010; Stranne and Björk, 2012; Wadhams et al., 2012).

The main data source for hemispheric sea ice thickness distribution is satellite radar altimetry. Laxon et al. (2003) used European Remote Sensing Satellite (ERS) 1/2 radar altimeter (RA) data to obtain a first estimate of Arctic Ocean sea ice thickness distribution. More recently Envisat and CryoSat-2 RA data has been used to compute sea ice thickness (Giles et al., 2008; Laxon et al., 2013). In a number of studies the retrieved sea ice freeboard and its derived thickness product were evaluated (e.g., Laxon et al., 2003; Giles and Hvidegaard, 2006; Giles et al., 2007; Connor et al., 2009). Yet to be calculated and evaluated is the sea ice thickness

using the combined time series of ERS-1/2 RA data and Environmental Satellite (Envisat) radar altimeter-2 (RA-2) data of the period 1993 to 2012.

Sea ice thickness can be obtained with other methods than radar altimetry. The Ice Cloud and Elevation Satellite (ICESat) with its Geophysical Laser Altimeter System (GLAS) allowed computing sea ice thickness from laser altimetry for up to three periods each year of about one month duration for years 2003 to 2009 (Kwok et al., 2009). Methods using active or passive microwave satellite sensor data (e.g. Kwok et al., 1995; Martin et al., 2004; Kaleschke et al., 2012) or using infrared satellite sensor data (e.g. Yu and Rothrock, 1996) do not allow computation of Arctic wide sea ice thickness distribution. These methods are limited in the maximum thickness to be retrieved, which is less than a meter, and can additionally be hampered by clouds. Note that also laser altimetry is influenced by clouds.

Ground-based, submarine-based, moored, and airborne sensors also provide sea ice thickness information via measurement of sea ice freeboard or total (sea ice plus snow) freeboard or sea ice draft. Such data form the basis of our current understanding of Arctic Ocean sea ice volume loss (Rothrock et al., 2008; Lindsay, 2010; Haas et al., 2008; 2011; Schweiger et al., 2011, Wadhams et al., 2011). On the one hand this data has limited spatial-temporal coverage in contrast to satellite remote sensing data. On the other hand this data is extremely valuable for validation of sea ice thickness products obtained from satellite observations.

We note that for all methods mentioned in the previous three paragraphs assumptions need to be made about, e.g., penetration depth of radar waves into the snow, ice and snow density, vertical sea ice structure, location of the dynamic sea surface height, and snow depth distribution. The only direct sea ice thickness measurement is a drill hole. Therefore it is important to keep in mind that products of the above-mentioned sources might have a bias and do have a finite uncertainty.

Within the SICCI project a selection of the most suitable retrieval methods and the most appropriate input data sets for freeboard-to-thickness conversion using radar altimeter data is carried out in the so-called Round Robin Exercise (RRE). This exercise is based on the analysis of data compiled in the Round Robin Data Package (RRDP). The RRDP comprises ERS-1/2 and Envisat RA data, input data required to convert sea ice freeboard into sea ice thickness and validation data of sea ice thickness, freeboard and draft as well as snow depth and total freeboard. The main goal of the RRE is not to validate a sea ice thickness product but rather to carry out a consistency check of the sea ice freeboard data obtained from satellite

RA. Another important part of the RRE is the investigation of the quality of the data used and the estimation of the sensitivity of the methods used to the input parameters. The goal is to find an optimal set of assumptions and input data for the freeboard-to-thickness conversion – assuming that the RA sea ice freeboard is correct. Validation of sea ice thickness obtained from these RA freeboard data will be carried out at a later stage of the SICCI project. This is the reason why a number of data sets one would expect to be used in this study, such as e.g. sea ice thickness derived from ICESat data or total (sea ice + snow) thickness derived from electromagnetic (EM) induction sounding are missing in the present study. For the same reason we did not use more recent Operation Ice Bridge (OIB) data.

The main objectives of this manuscript are A) to give insight into limitations of using a RA product with a grid resolution of the order of 100 km for sea ice thickness retrieval; B) to show the difficulties in using available independent data to choose the best suited parameter combination for freeboard-to-thickness conversion using the isostacy approach; C) to underline that we cannot yet quantify whether, e.g., usage of an ice-type dependent sea ice density yields a substantial improvement of sea ice thickness computed from freeboard estimates; D) to call for a consistent use of internationally agreed density values for freeboard-to-thickness conversion.

The paper is organized as follows: Sect. 2 describes the RRDP. Sect. 3 describes the methods used. In Sect. 4 we present the results of our analyses. These are discussed in Sect. 5 and concluded in Sect 6. We note that the results presented reflect the work of the SICCI project consortium and have been carried out at the respective institutions.

2 Data

This paper is based on data of the RRDP. These can be divided into two groups. The first group is used for sea ice thickness retrieval and comprises ERS-1/2 RA and Envisat RA-2 sea ice freeboard data, snow depth data from the Warren climatology (Warren et al., 1999), henceforth abbreviated with W99, and snow depth data from Advanced Microwave Scanning Radiometer aboard Earth Observation Satellite (AMSR-E) and Operation Ice Bridge (OIB) campaign flights. W99 also provides estimates of the snow density. The second group of data comprises the test and validation data for the RRE. These are basically data from moored, submarine, and airborne sensors as listed in Table 1.

2.1 Data for sea ice thickness retrieval

Sea ice freeboard data are derived from ERS-1/2 RA and Envisat RA-2 data using the methodology introduced by Laxon et al. (2003) and Giles et al. (2008) and described in detail in the SICCI ATBD (ESA SICCI project consortium, 2013). To shortly recap, elevation measurements from leads and ice floes are distinguished based on the pulse peakiness of the waveform. After re-tracking the range and applying necessary corrections (namely the Doppler range and delta Doppler, the ionospheric, the dry tropospheric and the modelled wet tropospheric, ocean tide, long-period tide, loading tide, earth tide, pole tide and inverse barometer corrections), and filters (removal of complex waveforms, failed re-tracking and echoes that yielded elevations more than 2 m from the mean dynamic sea surface height) the local sea level at ice floe locations is interpolated from nearby lead elevations. Freeboard is then calculated as the difference of radar altimetry measured ice floe elevation and the local sea level. Individual radar altimeter freeboard measurements are present in the RRDP data base. However, because a single freeboard measurement is known to be noisy, averaging several measurements is required. RA-2 freeboard estimates obtained along single orbits are averaged according to the co-location areas defined in section 2.2, or into a 2 degree longitude x 0.5 degree latitude grid (approximately 60 km grid cell size). Averaging is always done over one calendar month. Depending on latitude and number of leads identified, this results into about 20-150 measurements per grid cell.

W99 snow depth and density data is available as climatological monthly values for a given location. These are collocated individually for each single RA freeboard estimate and averaged over the same area and time as the freeboard (see above paragraph and section 2.2).

Figure 1 provides an overview of collocated RA-2 and W99 data for the Arctic Ocean for March and April 2010. The majority of RA-2 sea ice freeboard values are in a reasonable range. Only a few grid cells have negative sea ice freeboard (flagged black in Fig. 1 a, b). The W99 snow depth (Fig. 1 c, d) shows reasonable values for the Arctic Ocean. For the Bering Sea, the Hudson Bay, the Baffin Bay and parts of the Canadian Archipelago a decrease in W99 snow depth from March to April is observed together with a strong north-south gradient in the Baffin Bay. In these regions W99 snow depth is based on extrapolation. Figure 1 (e, f) illustrates the W99 snow densities for the Arctic Ocean for the same two months.

AMSR-E snow depth on sea ice data for the Arctic are taken from the AMSR-E/Aqua Daily L3 12.5 km Brightness Temperature, Sea Ice Concentration, & Snow Depth Polar Grids

product available from NSIDC (Cavalieri et al., 2004; http://nsidc.org/data/docs/daac/ae_si12_12km_tb_sea_ice_and_snow.gd.html). This data is provided at 12.5 km grid resolution as running 5-day mean and is limited to snow depth below 0.45 m on seasonal ice (Markus and Cavalieri, 1998; Comiso et al., 2003). The algorithm is sensitive to sea ice roughness (Worby et al., 2008, Ozsoy-Cicek et al., 2011; Kern et al., 2011) as well as snow wetness and grain size (Maksym and Markus, 2008; Markus and Cavalieri, 1998). Recently, AMSR-E snow depth data set quality was assessed for the Arctic (Cavalieri et al., 2012; Brucker and Markus, 2013). A comparison between OIB snow depth and AMSR-E snow depth for about 600 12.5 km grid cells between 2009 and 2011 (Brucker and Markus, 2013) indicated a basin average bias of up to 0.07 m and RMSE values between 0.03 m and 0.15 m. Under ideal conditions, i.e., for high concentration (> 90%) level first-year ice (FYI) thicker than 0.5 m the RMSE is below 0.06 m for, on average, 0.2 m thick snow (Brucker and Markus, 2013). For our study, AMSR-E snow depth is collocated with RA sea ice freeboard by averaging data over a calendar month over a disc of 100 km radius centred at each RA sea ice freeboard grid cell. We refer to section 2.2 for size of the co-location areas. For BGEP a 12 degree by 30 degree latitude-longitude box is used. This box may be oversized. The rationale behind using such a large co-location area was to maximize the number of valid RA freeboard estimates and to minimize the effect of sea ice motion changing ice type composition in that area.

2.2 Data for sea ice thickness validation and algorithm selection

The combination of a laser scanner and snow radar or a radar altimeter provides simultaneous collocated snow depth, snow freeboard and sea ice freeboard data. The laser scanner senses the snow surface and is used to derive the total freeboard – similar to the ICESat GLAS instrument – if the instantaneous sea surface height (SSH) is known. The snow radar directly measures snow depth on top of sea ice using the range difference between reflections at the two interfaces ice-snow and snow-air. For a radar altimeter operating at Ku-Band frequencies it is assumed that it provides the height of the ice-snow interface above the SSH: the sea ice freeboard, under dry snow and/or freezing conditions.

The RRDP includes a combination of CryoVEx laser scanner (ALS) and radar altimeter data (ASIRAS). ALS and ASIRAS data are taken from DTU Space, National Space Institute: ftp://ftp2.spacecenter.dk/pub/ESACCI-SI/ and are averaged over 50 km transects of flight line. The collocated RA-2 data are monthly averages of observations from all orbits within a

disc of 100 km radius centred at each ALS 50 km transect centre. We use data from campaigns at the end of April 2008 and beginning of May 2011. ALS data are used to derive total freeboard (Hvidegaard and Forsberg, 2002) with accuracy and precision of independent measurements of about 0.1 m to 0.15 m. ASIRAS sea ice freeboard data are derived using a method similar to Ricker et al. (2012) and have an accuracy of 0.15 to 0.2 m for independent measurements. As measurements are averaged along 50 km transects located in an area of frequent lead occurrence the accuracy relevant for this study is of the order of 0.01 m for the ALS data. For the same reason it can be expected that the accuracy of the ASIRAS data is better than the numbers given above and have a magnitude of 0.05 m to 0.1 m.

The RRDP includes OIB laser scanner (Airborne Thematic Mapper, ATM) and snow radar measured total freeboard, snow depth, and ice thickness (Panzer et al., 2013; Kurtz et al., 2013). OIB data are taken from the NSIDC: http://nsidc.org/data/icebridge/index.html and are averaged over 50 km transects along track. The collocated RA-2 data are monthly averages of observations from all orbits within a disc of 100 km radius centred at each OIB 50 km transect centre. We used data from OIB campaigns in April 2009 and March and April 2010. Kurtz et al. (2013) summarize the uncertainty sources of OIB snow depth retrieval. They point out that the results of Farrell et al. (2012) are a bit too optimistic: 0.01 m uncertainty in snow depth, and instead suggest a snow depth uncertainty of 0.06 m in agreement with Kwok et al. (2011): 0.03 m to 0.05 m for snow depths between 0.1 and 0.7 m. Lowest retrievable snow depth is of the magnitude 0.05 m.

Connor et al. (2009) report agreement of within 0.01 m between ATM measured total freeboard and sea ice freeboard for bare thin sea ice. Problems identified with the automatic SSH retrieval from ATM data alone for 2009 (Nathan Kurtz, personal communication, 2013) were mitigated starting with the 2010 OIB data by including contemporary digital imagery (Onana et al., 2013). In conclusion, for the bulk of total freeboard obtained from OIB ATM measurements the bias can be expected to be close to zero with an accuracy of between 0.05 m and 0.1 m (Farrell et al., 2012; Kurtz et al., 2013). This is confirmed by a study of Kwok et al. (2012) who found agreement between ICESat and OIB-ATM freeboards of within 0.01 m and a measurement repeatability of about 0.04 m.

Upward looking sonar (ULS) observes sea ice draft which can be converted into sea ice thickness in a similar way as the sea ice freeboard. In the RRDP we use data from the Beaufort Gyre ExPeriment (BGEP) where three, sometimes four moored ULS measured sea

ice draft. The approximate location of these moorings is denoted by the diamond in Fig. 2. BGEP ULS data are taken for years 2003 to 2008 from WHOI: http://www.whoi.edu/page.do?pid=66559. Accuracy of the data is estimated by Krishfield and Proshutinsky (2006) to be between 0.05 m and 0.1 m. This data is extremely valuable as it provides an independent measure of the seasonal cycle of sea ice draft and thus thickness. The collocated RA-2 data are monthly averages of observations from all orbits which fall into a box centred at the BGEP mooring location (see Fig. 2) extending over 12 degree latitude and 30 degree longitude.

Another source of ULS data in the RRDP are those carried on board submarines. Submarine ULS draft data were successfully used by Laxon et al. (2003) for a first assessment of Arctic Ocean sea ice thickness distribution obtained from ERS-1/2 data. The RRDP contains submarine ULS data from three cruises. Data from two of the cruises from U.S. submarines (April 1994 and October 1996) are available from NSIDC: http://nsidc.org/data/g01360.html. Data from the third cruise by a UK submarine (March/April 2007) are available from University of Cambridge (UCAM), see also (Wadhams et al., 2011). Submarine ULS data are in general less accurate than the BGEP data but are the only information about draft distribution over a larger region. Rothrock and Wensnahan (2007) report a bias of 0.29 m and a standard deviation of 0.25 m. An assessment of the UK submarine ULS data used reveals a standard deviation of 0.29 m and a bias of 0.4 m; these numbers are worse compared to the U.S. submarine data due to classified submarine positions. The collocated RA-2 data are monthly averages of observations from all orbits within a disc of 100 km radius centred at each submarine ULS 50 km transect centre. A transect length of 50 km is recommended by Rothrock and Wensnahan (2007).

Many other validation data are available, e.g. for ULS from submarines and the BGEP array, more recent OIB flight data, observations of total (sea ice + snow) thickness from electromagnetic (EM) sounding (Haas et al., 2008; 2010), and from ICESat (Kwok et al., 2009). The reason for not using this data for the present study lies in the nature of the project. We deliberately kept a large number of validation data for a later stage of the SICCI project to validate the prototype sea ice thickness product.

3 Methods

It is assumed that satellite radar altimetry measures the sea ice freeboard. By assuming isostasy, sea ice freeboard can be used to compute sea ice thickness z_i as follows:

$$z_i = \frac{z_s \rho_s + f_b \rho_w}{\rho_w - \rho_i} \quad (1)$$

with snow depth z_s, sea ice freeboard f_b, and the densities of sea water, sea ice and snow: ρ_w, ρ_i, and ρ_s, respectively. Figure 3 illustrates the parameters used in Eq. (1).

The main objectives of the RRE are

- To evaluate Eq. (1) for freeboard-to-thickness conversion.
- To select the best snow depth (product) for freeboard-to-thickness conversion.
- To investigate validity and influence of retrieval assumptions, like using constant sea ice density, on the sea ice thickness retrieval.

In order to achieve these goals the following investigations were carried out:

1. Snow depth data of the different data sets involved are inter-compared.
2. RA-2 sea ice freeboard is converted to snow freeboard and compared with OIB and CryoVEx snow freeboard.
3. RA and RA-2 sea ice freeboard is used to compute sea ice draft using different input data and compared to ULS sea ice draft data. This is done using our "standard set of densities" (see below). For BGEP mooring ULS data we compute in addition sea ice draft separately for MYI and FYI densities and two different fixed snow densities.
4. RA-2 sea ice freeboard is used to compute sea ice thickness combining the standard set of densities with various snow depth realizations and compared to OIB sea ice thickness.

The standard set of densities is: ρ_i = 900 kg m^{-3} (average density of MYI and FYI) and ρ_w = 1030 kg m^{-3} (Wadhams et al., 1992); snow density is taken from W99 and varies over space and time (see Fig. 1 e, f). In order to account for the effect of different densities for MYI and FYI (in 3, see above) we use sea ice densities published elsewhere (e.g., Timco and Frederking, 1996; Alexandrov et al., 2010): 882 kg m^{-3} and 917 kg m^{-3}, respectively. The two fixed snow density values used in 3 (see above) are 240 kg m^{-3} and 340 kg m^{-3} and correspond to the mean wintertime minimum and maximum snow density (Warren et al., 1999).

4 Results

In the following we present the results of comparing the various data sets. We start with snow depth and (sea ice) freeboard and then continue with sea ice draft and thickness.

4.1 Snow Depth

Snow depth is crucial for sea ice thickness estimation from altimeter data. Here we present results of our snow depth inter-comparison. Figure 4 shows snow depth data available for CryoVEx (image a and c) and from OIB data (image b) in the Fram Strait area. Because ASIRAS and ALS both sensed the snow-air interface (see Sect. 4.2) no additional snow depth observations other than W99 and those retrieved using AMSR-E data over FYI are available for 2008 and 2011. Mean snow depth values given underneath Fig. 4 illustrate that W99 snow depth values are more than twice as large as OIB or AMSR-E snow depths.

Figure 5 shows the distribution of OIB snow depth (image a) and its difference to W99 (image c) and AMSR-E (image e) snow depths for April 2010 for the Arctic Ocean. It illustrates that over FYI (Fig. 5 e) OIB and AMSR-E snow depths agree within 0.05 m while OIB underestimates W99 snow depth over FYI by about 0.21 m and over MYI by about 0.11 m (Fig. 5 c). These results are summarized in Table 2 together with the results for 2009. In 2009 OIB underestimates W99 snow depth over FYI by a 0.19 m, similar to 2010. The agreement with W99 snow depth over MYI is much better with a difference of just 0.02 m. Fig. 5 e) illustrates that in April 2010 OIB flights tracks are located over FYI in the Arctic Ocean and in the Canadian Archipelago. For the latter region we only compare OIB and AMSR-E snow depth data in the following because W99 snow depth and density data rely solely on extrapolation in this region. The same applies to the Fram Strait area (see Figure 4). However, the sea ice cover in the Fram Strait area is quite dynamic and originates from the Arctic Ocean while the sea ice cover in the Canadian Archipelago is much more static. Hence it can be assumed that at least during winter sea ice and snow properties in the Fram Strait area are similar to those upstream in the Arctic Ocean, which is actually confirmed by the W99 data (not shown), while those in the Canadian Archipelago are determined by local processes and the sea ice which entered the region during the previous summer season.

The right hand column of images in Fig. 5 compares AMSR-E snow depth with OIB snow depth for FYI in the Arctic Ocean; data from the Canadian Archipelago are excluded. Figure 5 b) suggests that W99 snow depths are twice as large as AMSR-E ones over FYI in the

Arctic Ocean; the difference is 0.18 m (Table 2). However, even though AMSR-E and OIB snow depths seem to agree well, a linear regression analysis points to a correlation of -0.121, i.e. a poor agreement. Figure 5 d) suggests two different snow density regimes. Agreement improves substantially when we limit the comparison to data pairs with W99 snow density above 320 kg m^{-3}, which is the typical snow density in March / April (Warren et al., 1999), with a correlation of 0.83, a slope of 1.19 and bias of 0.0 m. AMSR-E snow depth retrieval reliability depends on FYI fraction. Figure 5 f) illustrates how much the FYI fraction varies for the data set considered. Limitation of the comparison to cases with > 95% FYI fraction, results in improved agreement between AMSR-E and OIB snow depth, with a correlation of 0.76, a slope of 0.74, a bias of 0.06 m and a mean difference of 0.03 m. The results are similar for 2009 (not shown).

For the Canadian Archipelago, OIB and AMSR-E snow depth agree with each other with a correlation of 0.70 and a mean difference of 0.01 m (see Table 2, rightmost column), however slope and bias of the linear regression are 0.43 and 0.08 m. Here we investigate the land-spill over effect because grid cells with contributions from sea ice and land to the measured brightness temperatures can influence AMSR-E snow depth retrieval. We find that limitation to 100 km resolution grid cells with low or zero land fraction does not improve the result of the regression.

The results of our snow depth comparison agree with Kurtz and Farrell (2011) and Kurtz et al. (2013): Over FYI AMSR-E data give a much better measure of the actual snow depth than W99; the latter are about twice as large as AMSR-E and OIB snow depths over FYI. Over MYI, OIB and W99 differ by only 0.02 m in 2009 but by 0.12 m in 2010. Only grid cells with at least 65% MYI are used here. One possible explanation for the different degree of agreement could be inter-annual variation in snow depth over MYI. While in 2009 OIB snow depth was 0.36 m it was just 0.23 m in 2010. Mean W99 snow depth was 0.35 m and 0.34 m, respectively. It could be that the W99 snow depth climatology does not capture the inter-annual variability in snow depth over MYI in the Arctic Ocean. The investigation should be extended to more years to confirm this statement.

4.2 Sea Ice and Total Freeboard

During the CryoVEx campaigns in 2008 and 2011 in the Fram Strait both the radar altimeter (ASIRAS) and the laser instrument (ALS) essentially sensed the snow surface. Radar

penetration into the snow cover on sea ice in the Fram Strait during CryoVEx campaigns was close to zero although the radar is supposed to sense the ice-snow interface at the used frequency in Ku-Band according to laboratory experiments (Beaven et al., 1995). There is growing evidence that this assumption does not hold for more cases than previously thought (e.g. Ricker et al., 2014). Both freeboard measurements (ASIRAS and ALS) linearly agreed with a RMSD of 0.02 m, a bias of about 0.05 m, a slope close to 1 and a linear correlation coefficient of 0.99 for 2008 and 2011. Therefore from CryoVEx only total freeboard is used in this study. For 2011, CryoVEx ALS total freeboard underestimates RA-2 total freeboard computed using W99 snow depth by 0.06 m; for 2008, this underestimation is about 0.16 m. These values are larger than the uncertainties expected for transect lengths of 50 km for the ALS data. It has to be kept in mind that we look at 21 and 11 data pairs only, respectively.

OIB total freeboard observations are compared with RA-2 total freeboards computed from RA-2 sea ice freeboard and OIB or W99 snow depth in the Arctic Ocean (Table 3, Figure 6). Mean OIB total freeboard in the Arctic Ocean agrees overall within 0.02 m with RA-2 total freeboard when using collocated OIB snow depths. If instead W99 snow depth is used the agreement remains fine for 2009 but for 2010 RA-2 underestimates the overall mean OIB snow freeboard by 0.11 m. This can be explained by the difference between OIB snow depth and W99 snow depth (see Sect. 4.1) but also by the different fraction of MYI in these data sets. For 2009 snow depth and total freeboard are available from OIB only over MYI while for 2010 about one third of the OIB data were obtained over FYI (see Fig. 5). As shown in Sect. 4.1, OIB snow depth agrees much better with W99 snow depth over MYI than over FYI.

4.3 Sea Ice Draft

The results of the comparison of sea ice draft between ULS and radar altimeter is summarized in Table 4. Sea ice draft observed by U.S. submarine ULS in October 1996 is overestimated by ERS-1 RA by 0.13 m which is within the ULS uncertainty of 0.25 to 0.3 m. For April 1994, however, ERS-1 RA underestimates observed sea ice draft by 0.45 m which is outside the uncertainty range given for these ULS data. This discrepancy is illustrated in Fig. 7 c) and d): While both data sets show maximum probability in the same draft bin of 1.5 to 2.0 m for 1996, the histograms are shifted relative to each other for 1994 with largest probability in bin 2.5 to 3.0 m for the ULS data but 2.0 to 2.5 m for RA data. The scatterplot in Fig. 7 e) underlines that the agreement is much better for 1996 than for 1994; in particular the RMSD for 1996 is less than half the one for 1994.

Sea ice draft observed by UK submarine ULS in April 2007 is underestimated by RA-2 by 0.12 m (Table 4). However, the majority of this cruise took place north of the northern limit of RA-2 data coverage and therefore is based on only 15 data pairs, compared to about 90 and 40 data pairs for the U.S. submarine cruises.

Mean winter sea ice draft observed by BGEP ULS agrees within 0.05 m with sea ice draft computed from RA-2 data using W99 snow depth and density and standard sea ice and water density values. However, the seasonal range in sea ice draft is much lower for RA-2 than for BGEP ULS (Table 4, Fig. 8). Only for winters 2005/2006 and 2006/2007 does the seasonal range of sea ice draft agree in both data sets. The area considered here was covered by almost 100% MYI from 2003 to 2007 (first four winters), whereas FYI entered the region in winter 2007/2008 (taken from AMSR-E snow depth data set, Cavalieri et al., 2004). Therefore, for the first four winters, one might need to use the MYI density instead of the value of 900 kg m^{-3} used. By doing so the RA-2 draft would decrease by between 0.1 m and 0.4 m, depending on season and year (Fig. 8, brown lines). This results in a better agreement between BGEP ULS and RA-2 draft early in the winter season, but it does not improve agreement in terms of the seasonal range. Note that usage of AMSR-E snow depth, possible for winter 2007/2008, results in RA-2 draft values that would be typical for 100% MYI and a snow density of about 290 kg m^{-3} (Fig. 8, green dots). However, AMSR-E snow depth can only be obtained over FYI so one might need to use the FYI density of 917 kg m^{-3}. This would shift the green dots by 0.3 m towards larger ice draft values (Fig. 8, compare blue and black lines) and would thus cause a slightly better agreement between ULS and RA-2 drafts. More investigations are needed to confirm this.

4.4 Sea Ice Thickness

Sea ice thickness is computed from RA-2 data using different snow depth data and compared to OIB (2009, 2010) sea ice thickness estimates. We omitted CryoVEx data from this comparison because of the ambiguous results reported in Sect. 4.2 and because W99 snow depth is potentially less reliable in the area sensed during CryoVEx compared to OIB 2010 (see Fig. 4). Snow depth data sets used are W99 only, W99 over MYI and 0.5 x W99 over FYI (Kurtz and Farrell (2011), henceforth abbreviated KF11), OIB only, and W99 over MYI but AMSR-E over FYI. The results of this comparison are summarized in Table 5 for the Arctic Ocean and in Table 6 for the Fram Strait.

For OIB 2009 data of the Arctic Ocean, none of the four snow data sets reveals a RA-2 sea ice thickness correlated with the OIB one better than 0.65. Using OIB snow depth gives highest correlation and smallest RMSE of 0.96 m. However, RMSD is similar for the other three data sets. For OIB 2010 data of the Arctic Ocean, using OIB snow depth gives highest correlation but largest RMSE: 0.38 and 1.52 m (Table 5). Correlations and RMSD are smaller when using the other snow data sets. Using W99 data results in lowest correlation but also the smallest RMSD (Table 5). This is illustrated by Fig. 9 which shows scatter plots of sea ice thickness computed using the mentioned snow depth data sets versus observed sea ice thickness during OIB for 2009 (images a to c) and 2010 (images d to f). Using W99 in combination with AMSR-E and KF11 results in a similar statistics because AMSR-E snow depth is found to be close to half the W99 snow depth and to be in agreement with OIB snow depth within 0.02 m (see Table 1 and Kurtz and Farrell (2011)).

For the Fram Strait, OIB and RA-2 sea ice thickness agree with each other similarly well using OIB 2010 or W99 snow depth data: the correlation is 0.84 and 0.80, respectively (Table 6). Similar to 2010 in the Arctic Ocean (Table 5) the RMSD is smaller using W99 snow depth: 0.88 m, than using OIB snow depth: 1.03 m. The number of data points is, however, substantially smaller in this region than in the Arctic Ocean region: only 13 data pairs (Figure 9 g, h) which limits the value of this comparison.

5 Discussion

We compared ULS sea ice draft with sea ice draft computed from RA sea ice freeboard using six different realizations of the freeboard-to-draft conversion. Of the six realizations one uses fixed ice density at 900 kg m^{-3} , i.e. the average of typical FYI and MYI densities, and W99 snow depth (A1); one uses separate FYI and MYI densities and parameterizes W99 snow depth following (Laxon et al., 2013) (A2); one uses fixed FYI density at 910 kg m^{-3} combined with a freeboard dependent MYI density (Ackley et al., 1974) and W99 snow depth (A3); one uses fixed ice density at 900 kg m^{-3} (see A1) with full and half W99 snow depth over FYI and MYI, respectively (A4); one uses separate but fixed FYI and MYI snow depth and separate FYI and MYI densities (Alexandrov et al., 2010) (A5); one follows the empirical approach for thick MYI without including any snow depth information (Wadhams et al., 1992) (A6). All realizations use seasonally varying W99 snow density. Of these realizations only A1 is shown in Figures 7 and 8. Table 7 summarizes the difference in the mean and median observed

minus computed sea ice draft (SID) for the six realizations and the ULS data sets listed in Table 1.

We note here that almost all SID data and many of our validation data are from MYI regions. A real assessment of approaches which include ice-type dependent ice density and snow depth could therefore not be carried out in a systematic enough way. More work and more data are required here.

Our main conclusion from the comparison is that A1, A3 and A4 are agreeing equally well with the ULS SID data within their uncertainty bounds (about 0.3 m for BS and BSS and 0.05 m for BGEP), and that A5 and A6 show the largest discrepancies. Why is A2 (Laxon et al., 2013) biased low? Almost all ULS data are obtained under MYI (see above). A2 uses a MY ice density of 882 kg m^{-3} while A1 and A4 use 900 kg m^{-3}. Such a difference in sea ice density can cause a negative bias in the obtained SID by 0.2 m (compare blue and brown lines in Fig. 8). However, the good agreement between A1 and A4 in mean and median SID (Table 7) does not mean these use the perfect input parameter combination. As we can see in Figure 8 for A1, agreement between observed and computed SID varies from month to month. RA-2 SID does not very well capture the increase in ULS SID. Generally the increase in RA-2 SID is smaller than the increase in ULS SID. This can have various reasons.

The area covered by the BGEP moorings (A, B, C and D) is approximately 4 degrees in latitude by 10 degrees in longitude while RA-2 SID is computed from an area of 12 degrees in latitude by 30 degrees in longitude to account for ice type changes due to drift during the course of the freezing season. Hence RA-2 SID is an average over an almost 10-fold larger area which can explain the smaller seasonal amplitude.

We assume that RA-2 sea ice freeboard and OIB snow depth and total freeboard can be combined on the spatiotemporal scales used (100 km, daily vs. monthly). We use OIB snow depth to compute a RA-2 total freeboard and compare it with OIB total freeboard. These two data sets agree within 0.02 m. Conversely, an estimate of sea ice freeboard from OIB obtained by subtracting OIB snow depth from OIB total freeboard agrees within 0.02 m with RA-2 sea ice freeboard. This is better than the accuracy of 0.05 m given for RA-2 and OIB freeboard data (Kurtz et al., 2013) and is an indication that at least along OIB tracks in 2009 and 2010 in the Arctic Ocean Envisat RA-2 sea ice freeboard is within a reasonable range.

We find that typical variations in sea ice density cause variations in sea ice thickness that are as large as those caused by snow depth variations. This is different to laser altimetry (Kwok

and Cunningham (2008). Under typical variations we understand the difference between MY and FY ice densities (Alexandrov et al., 2010) and the difference between snow depth on MYI compared to FYI (see Table 2). For typical sea ice freeboard values, uncertainties in sea ice thickness between 0.4 and 0.8 m can be expected. For typical snow density variations, sea ice thickness uncertainties stay at around 0.2 to 0.3 m. These values are confirmed by Fig. 8 which reveals differences of up to 0.7 m (March 2004 and March 2005) between RA-2 SID calculated with typical values for FYI densities (black lines) and MYI densities (brown lines).

W99 snow depth is twice as large as OIB snow depth over FYI, in agreement with Kurtz and Farrell (2011) and Kurtz et al. (2013), which is confirmed by AMSR-E snow depths agreeing with OIB snow depth within 0.02 m. This finding might not be too relevant for the comparison shown in Figure 8 because the larger part of the area used for RA-2 SID computations for the BGEP region was covered by MYI. However, we find that even over MYI W99 might over-estimate the actual snow depth, as is the case for April 2010. More snow depth inter-comparisons are required to further investigate this finding. Also, a better quantification of the actual MYI fraction in the BGEP region using a different MYI fraction data set than the one inherent in the AMSR-E snow depth product would be required.

A detailed investigation of the impact of snow density is not carried out. According to the W99 climatology and other studies, e.g. Alexandrov et al. (2010), snow density varies seasonally between < 100 kg m^{-3} (fresh snow) to > 400 kg m^{-3} (old, compacted snow). Snow density can also vary on short spatial scales. However, in this study satellite RA data is used to obtain sea ice thickness at 100 km spatial scale and a temporal scale of a month. Therefore we feel confident to refer to Fig. 8 to illustrate the effect of snow density which we vary over the range of values given in W99: 240 to 340 kg m^{-3}. The change in mean SID associated with the snow density range applied is about 0.2 to 0.3 m. This translates into a bias in sea ice thickness of a magnitude of 0.3 m and suggests to use seasonally varying snow density when retrieving ice thickness from satellite RA data as is done in this paper.

It is important to bear in mind the different spatiotemporal scales which are involved. For instance, OIB data is obtained at fine spatiotemporal resolution along transects and is averaged over 50 km long segments for this study (see section 2.2). RA-2 data, as are used here, comprise measurements from all overpasses within a month which fall into a disc of 100 km diameter centred at each 50 km OIB track segment. In addition the footprint of a single RA-2 measurement is 1-2 orders of magnitude larger than the footprint of a single OIB

measurement. It is likely that RA-2 data provide an average ice thickness rather than the actual range of ice thickness values (see Fig. 9). This depends, however, on the degree by which different ice types and ice surface properties impact the radar backscatter and the waveform (Zygmuntowska et al., 2013, Ricker et al., 2014). More studies need to look into the different backscatter of sea ice of different type and roughness to quantify the impact of sea ice property variation on the radar altimeter signal and hence the sea ice freeboard.

OIB sea ice thickness is computed using a fixed sea ice density of 915 kg m^{-3} (Kurtz et al., 2013). This density value represents FYI but results in a positive bias in draft and thickness for MYI because it is about 30 kg m^{-3} higher than the average MYI density value suggested, e.g., by Alexandrov et al. (2010). This makes an assessment of the obtained sea ice thickness values a difficult task, in particular if the aim is to quantify the impact of different sea ice density values on the obtained sea ice thickness. Currently, OIB data are the only airborne data source for contemporary data of freeboard and snow depth.

Our interpretation of the CryoVEx data remains inconclusive because the ASIRAS instrument, which is supposed to sense the ice-snow interface and thus provide an independent sea ice freeboard measurement, failed to do so. Instead it provided the total freeboard like the ALS sensor. By means of atmospheric re-analysis data we identify snow cover property changes as a possible reason for CryoVEx data from 2011 but not for 2008. This suggests that even under freezing conditions sensors like Envisat RA-2 or Cryosat-2 might not sense the sea ice surface. It is likely, that vertical snow density gradients and/or volume scattering in the snow in general influence the radar signal, resulting in a less distinct signal from the ice-snow interface or in similarly strong returns from the snow surface or interior as was shown for Antarctic sea ice by Willatt et al., (2010).

6 Summary and Recommendations

Satellite radar altimetry (RA) has been providing surface elevation measurements of the Arctic Ocean for about two decades. With the assumption that these elevation measurements represent sea ice freeboard these are used to derive sea ice thickness (Laxon et al., 2013; 2003). Here we report about first results of an investigation about uncertainties involved in RA freeboard-to-thickness conversion carried out within the European Space Agency Climate Change Initiative sea ice Essential Climate Variable project using Envisat radar altimetry (RA-2). For uncertainty estimation of and recent advances in sea ice freeboard retrieval using

RA data, which is not part of the present paper, we refer to, e.g., Zygmuntowska et al. (2013); Ricker et al. (2014); Kurtz et al. (2014) and Armitage and Davidson (2014).

We found the Warren snow depth climatology (W99, Warren et al., 1999) to be outdated, in agreement with earlier studies (Kwok et al., 2011; Kurtz and Farrell, 2011). Modal and mean sea ice draft computed from RA-2 sea ice freeboard using different realizations of the freeboard-to-draft conversion agree with upward looking sonar observations of winter (Oct.-Mar.) sea ice draft in the Beaufort Sea within the uncertainty bounds – provided the realizations include spatiotemporally varying snow depth and density. None of the realizations is able to re-produce the seasonal range in sea ice draft. A change of sea ice densities and/or snow depths as a function of ice type can improve the agreement at the beginning or end of the freezing season but seems not to have an impact on the overall seasonal sea ice draft range obtained from RA-2 data. Sea ice thickness computed from RA-2 sea ice freeboard using different snow depth data sets over-estimate (under-estimate) small (large) OIB sea ice thickness. An improvement from using ice type dependent snow depth is not evident but most likely needs more data and a different inter-comparison strategy to be quantified.

Some of the independent data used in our study point towards a larger range in sea ice draft and thickness than observed by RA-2. This results from the impact of different ground resolutions of the compared sensors. Also, averaging over a track length of 50 km or 100 km of a submarine or an airborne sensor can only be an approximation of the variability in sea ice freeboard obtained from RA-2 over a disc with diameter 100 km. Data from submarine and airborne campaigns cover a few days while RA-2 data are averages over a month. More emphasis needs to be put on the choice of the scales involved both for sea ice thickness computation and validation. We note that our motivation in this study is the need to evaluate a monthly 100 km spatial scale sea ice thickness product.

Hence, for a better validation of both sea ice freeboard and thickness products at such a spatiotemporal scale more data from airborne campaigns are required. Data from airborne campaigns, which allow sea ice thickness retrieval, often suffer from i) environmental conditions and their not yet fully known impact on snow and sea ice physical properties, e.g. CryoVEx 2008 and 2011; ii) uncertainty sources are not yet well understood (Kurtz et al., 2013); iii) assumptions and parameters, such as sea ice and snow densities, used for derivation of sea ice thickness or snow from air-borne data may differ from campaign to campaign and

to space-borne data, and may not be state-of-the-art in view of recent literature (e.g. Alexandrov et al., 2010; Laxon et al., 2013).

We formulate the following recommendations for freeboard-to-thickness conversion using radar altimetry for the Arctic Ocean:

1. The Warren Climatology has to be used carefully. It is not valid over first-year ice and it is of limited use outside the Arctic Ocean. It is recommended to use the Warren Climatology in combination with a second data set of snow depth over first-year ice.

2. Using radar altimetry, the impact of sea ice density on sea ice thickness retrieval is as large as the impact of snow depth. Recent studies indicate that the difference in sea ice densities of multiyear ice and first-year ice is large enough to explain sea ice thickness under- or over-estimations of the order of 0.5 m or more. It is recommended to use an ice-type dependent set of sea ice densities. In addition it is important to also consider the density difference between ridged and level ice. We need many more measurements of ice density and isostasy across first-year ice and multiyear ice ridges to derive area-averaged ice densities for ridged sea ice.

3. For a sophisticated inter-comparison and validation of the final sea ice thickness product from satellite altimetry it is mandatory to use independent and preferably non-altimetric validation data. The amount of such contemporary sea ice draft, snow depth and sea ice thickness data is clearly sub-optimal and needs to be improved.

4. Potential improvement from utilizing new sets of input parameters, e.g. densities, cannot be quantified without consistent input parameters for freeboard-to-thickness conversion. We call for a consistent internationally agreed standard set of densities to be used for freeboard-to-thickness conversion to be applied to air- and spaceborne altimeter data.

Acknowledgements

This work was funded by ESA/ESRIN (Sea Ice CCI). S. Kern acknowledges support from Center of Excellence for Climate System Analysis and Prediction (CliSAP), University of Hamburg, Germany. We are grateful to numerous data providers for the present study, namely: National Snow and Ice Data Centre (NSIDC) for OIB data, AMSR-E snow depth, SSM/I and AMSR-E sea ice concentrations, and the U.S. submarine ULS data; Woods Hole Oceanographic Institute for BGEP ULS data; ESA for re-processed ERS-1/2 and Envisat ASAR data. The authors are grateful to all the teams in the field, in the air and in the ship for

providing all these valuable observations. S. Kern acknowledges support from the International Space Science Institute (ISSI), Bern, Switzerland, under project # 245: Heil, P., and, S. Kern, “Towards an Integrated Retrieval of Antarctic Sea Ice Volume”. We thank the efforts of three anonymous reviewers and our editor Julienne Stroeve to improve the paper.

References

Ackley, S. F., Hibler III, W. D., Kugzruk, F., Kovacs, A., and Weeks, W. F.: Thickness and roughness variations of Arctic multiyear sea ice, AIDJEX Bulletin, 25, 75-95, 1974.

Alexandrov, V., Sandven, S., Wahlin, J., and Johannessen, O. M.: The relation between sea ice thickness and freeboard in the Arctic, The Cryosphere, 4, 373-380, 2010.

Armitage, T. W. K. and Davidson, M. W. J.: Using the interferometric capabilities of the ESA Cryosat-2 mission to improve the accuracy of sea ice freeboard retrievals, Trans. Geosci. Rem. Sens., 51(1), 529-536, doi: 10.1109/TGRS.2013.2242082, 2014.

Brucker, L. and Markus, T.: Arctic-Scale Assessment of Satellite Passive Microwave Derived Snow Depth on Sea Ice using Operational IceBridge Airborne Data, J. Geophys. Res. – Oceans, 118, doi:10.1002/ jgrc.20228, 2013.

Cavalieri, D. J., Markus, T., and Comiso, J. C.: AMSR-E/Aqua Daily L3 25 km Brightness Temperature & Sea Ice Concentration Polar Grids Version 2, Boulder, Colorado USA: NASA DAAC at the National Snow and Ice Data Center, 2004.

Cavalieri, D. J., Markus, T., Ivanoff, A., Miller, J. A., Brucker, L., Sturm, M., Maslanik, J., Heinrichs, J. F., Gasiewski, A. J., Leuschen, C., Krabill, W., and Sonntag, J.: A Comparison of Snow Depth on Sea Ice Retrievals Using Airborne Altimeters and an AMSR-E Simulator, Trans. Geosci. Rem. Sens., 50(8), 3027-3040, 2012.

Comiso, J. C.: Large decadal decline of the Arctic multiyear ice cover, J. Clim., 25, 1176-1193, 2012.

Comiso, J. C., Cavalieri, D. J., and Markus, T.: Sea ice concentration, ice temperature and snow depth using AMSR-E data, Trans. Geosci. Rem. Sens., 41(2), 243-252, 2003.

Connor, L. N., Laxon, S. W., Ridout, A. L., Krabill, W., and McAdoo, D.: Comparison of Envisat radar and airborne laser altimeter measurements over Arctic sea ice, Rem. Sens. Environ., 113, 563–570, 2009.

ESA SICCI project consortium: D2.6: Algorithm Theoretical Basis Document (ATBDv1), ESA Sea Ice Climate Initiative Phase 1 Report SICCI-ATBDv1-04-13, version 1.1, 2013.

Farrell, S. L., Kurtz, N. T., Connor, L., Elder, B., Leuschen, C., Markus, T., McAdoo, D. C., Panzer, B., Richter-Menge, J., and Sonntag, J.: A First Assessment of IceBridge Snow and Ice Thickness Data over Arctic Sea Ice, Trans. Geosci. Rem. Sens., 50, 6, 2098-2111, 2012.

Forstrøm, S., Gerland, S., and Pedersen, C.: Thickness and density of snow-covered sea ice and hydrostatic equilibrium assumption from in situ measurements in Fram Strait, the Barents Sea and the Svalbard coast, Ann. Glaciol., 52(57), 261-271, 2011.

Giles, K. A. and Hvidegaard, S. M.: Comparison of space borne radar altimetry and airborne laser altimetry over sea ice in the Fram Strait, Int. J. Rem. Sens., 27, 3105-3113, 2006.

Giles, K. A., Laxon, S. W., Wingham, D. J., Wallis, D. W., Krabill, W. B., Leuschen, C. J., McAdoo, D., Manizade, S. S., and Raney, R. K.: Combined airborne laser and radar altimeter measurements over the Fram Strait in May 2002, Rem. Sens. Environ., 111, 182–194, 2007.

Giles, K. A., Laxon, S. W., and Ridout, A. L.: Circumpolar thinning of Arctic sea ice following the 2007 record ice extent minimum, Geophys. Res. Lett., 35, L22502, doi:10.1029/2008GL035710, 2008.

Haas, C., Pfaffling, A., Hendricks, S., Rabenstein, L., Etienne, J.-L., and Rigor, I.: Reduced ice thickness in Arctic Transpolar Drift favours rapid ice retreat, Geophys. Res. Lett., 35, L17501, doi:10.1029/2008GL034457, 2008.

Haas, C., Hendricks, S., Eicken, H., and Herber, A.: Synoptic airborne thickness surveys reveal state of Arctic sea ice cover, Geophys. Res. Lett., 37, L09501, doi:10.1029/2010GL042652, 2010.

Hvidegaard, S. M. and Forsberg, R.: Sea ice thickness from laser altimetry over the Arctic Ocean north of Greenland, Geophys. Res. Lett., 29(20), 1952-1955, 2002.

Kaleschke, L., Tian-Kunze, X., Maaß, N., Mäkynen, M., and Drusch, M.: Sea ice thickness retrieval from SMOS brightness temperatures during the Arctic freeze-up period, Geophys. Res. Lett., 39, L05501, 2012.

Kern, S., Ozsoy-Cicek, B., Willmes, S., Nicolaus, M., Haas, C., and Ackley, S. F.: An intercomparison between AMSR-E snow depth and satellite C- and Ku-Band radar backscatter data for Antarctic sea ice, Ann. Glaciol., 52(57), 279-290, 2011.

Krinner, G., Rinke, A., Dethloff, K., and Gorodetskaya, I. V.: Impact of prescribed Arctic sea ice thickness in simulations of the present and future climate, Clim. Dyn., 35, 619-633, doi:10.1007/s00382-009-0587-7, 2010.

Krishfield, R. and Proshutinky, A.: BGOS ULS Data Processing Procedure Report, http://www.whoi.edu/fileserver.do?id=85684&pt=2&p=100409, Woods Hole Oceanographic Institute, 2006.

Kurtz, N. T. and Farrell, S. F.: Large-scale surveys of snow depth on Arctic sea ice from Operation IceBridge, Geophys. Res. Lett., 38, L20505, doi:10.1029/2011GL049216, 2011.

Kurtz, N. T., Farrell, S. L., Studinger, M., Galin, N., Harbeck, J., Lindsay, R., Onana, V., Panzer, B., and Sonntag, J. G.: Sea ice thickness, freeboard, and snow depth products from Operation IceBridge airborne data, The Cryosphere, 7, 4771–4827, 2013.

Kurtz, N. T., Galin, N., and Studinger, M.: An improved CryoSat-2 sea ice freeboard and thickness retrieval algorithm through use of waveform fitting, The Cryophere Disc., 8, 721-768, doi:10.5194/tcd-8-721-2014, 2014.

Kwok, R. and Cunningham, G. F.: ICESat over Arctic sea ice: Estimation of snow depth and ice thickness, J. Geophys. Res., 113, C08010, 2008.

Kwok, R., Nghiem, S. V., Yueh, S. H., and Huynh, D. D.:, Retrieval of Thin Ice Thickness from Multifrequency Polarimetric SAR Data, Rem. Sens. Environ., 51(3), 361-374, 1995.

Kwok, R., Cunningham, G. F., Wensnahan, M., Rigor, I., Zwally, H. J., and Yi, D.: Thinning and volume loss of the Arctic Ocean sea ice cover: 2003–2008, J. Geophys. Res., 114, C07005, 2009.

Kwok, R., Panzer, B., Leuschen, C., Pang, S., Markus, T., Holt, B., and Gogineni, S. P.: Airborne surveys of snow depth over Arctic sea ice, J. Geophys. Res., 116, C11018, 2011.

Kwok, R., Cunningham, G. F., Manizade, S. S., and Krabill, W. B.: Arctic sea ice freeboard from IceBridge acquisitions in 2009: Estimates and comparisons with ICESat, J. Geophys. Res., 117, C02018, 2012.

Laxon, S., Peacock, N., and Smith, D.: High interannual variability of sea-ice thickness in the Arctic region, Nature, 425, 947–950, 2003.

Laxon, S. W., Giles, K. A., Ridout, A. L., Wingham, D. J., Willatt, R., Cullen, R., Kwok, R., Schweiger, A., Zhang, J., Haas, C., Hendricks, S., Krishfield, R., Kurtz, N., Farrell, S. L., and

Davidson, M.: CryoSat-2 estimates of Arctic sea ice thickness and volume, Geophys. Res. Lett., 40, 1–6, 2013.

Lindsay, R., New unified sea ice thickness climate data record, EOS, 91(44), 405-406, 2010.

Maksym, T. and Markus, T.: Antarctic sea ice thickness and snow-to-ice conversion from atmospheric reanalysis and passive microwave snow depth, J. Geophys. Res., 113, C02S12, doi:10.1029/2006JC004085, 2008.

Markus, T. and Cavalieri, D. J.: Snow depth distribution over sea ice in the southern ocean from satellite passive microwave data, In: Antarctic Sea Ice: Physical Processes, Interactions, and Variability, M. O. Jeffries (Ed.), AGU Antarctic Research Series, 74, 19-39, 1998.

Martin, S., Drucker, R., Kwok, R., and Holt, B.: Estimation of the thin ice thickness and heat flux for the Chukchi Sea Alaskan coast polynya from Special Sensor Microwave/ Imager data,1990–2001, J. Geophys. Res., 109, C10012, doi:10.1029/2004JC002428, 2004.

Onana, V.-de-P., Kurtz, N. T., Farrell, S. L., Koenig, L. S., Studinger, M., and Harbeck, J. P.: A sea-ice lead detection algorithm for use with high-resolution airborne visible imagery, Trans. Geosci. Rem. Sens., 51(1), 38-56, 2013.

Panzer, B., Gomez-Garcia, D., Leuschen, C., Paden, J., Rodriguez-Morales, F., Patel, A., Markus, T., Holt, B., and Gogineni, S. P.: An ultra-wideband, microwave radar for measuring snow thickness on sea ice and mapping near-surface internal layers in polar firn, J. Glaciology, 59(214), 244-255, 2013.

Ricker, R., Hendricks, S., Helm, V., Skourup, H., and Davidson, M.: Sensitivity of CryoSat-2 Arctic sea-ice volume trends on radar-waveform interpretation, The Cryosphere Discuss., 8, 1831-1871, doi:10.5194/tcd-8-1831-2014, 2014.

Ricker, R., Hendricks, S., Helm, V., Gerdes, R. and Skourup, H.: Comparison of sea-ice freeboard distribution from aircraft data and CryoSat-2, Proceedings paper, 20 years of progress in radar altimetry, 24-29 Sep., Venice, Italy, 2012.

Rothrock, D. A. and Wensnahan, M.: The accuracy of sea-ice drafts measured from U.S. Navy submarines, J. Atmos. Ocean. Technol., 24, doi:10.1175/JTECH2097.1, 2007.

Rothrock D. A., Percival, D. B., and Wensnahan, M.: The decline in arctic sea-ice thickness: separating the spatial, annual, and interannual variability in a quarter century of submarine data, J. Geophys. Res., 113, C05003, doi:10.1029/2007JC004252, 2008.

Schweiger, A., Lindsay, R., Zhang, J., Steele, M., Stern, H., and Kwok, R.: Uncertainty in modeled Arctic sea ice volume, J. Geophys. Res., 116, C00D06, doi:10.1029/2011JC007084, 2011.

Spreen, G., Kern, S., Stammer, D., Forsberg, R., and Haarpaintner, J.: Satellite based estimation of sea ice volume flux through Fram Strait, Ann. Glaciol., 44, 321-328, 2006.

Stranne, C. and Björk, G.: On the Arctic Ocean ice thickness response to changes in external forcing, Clim. Dyn., 39, 3007-3018, doi:10.1007/s00382-011-1275-y, 2012.

Wadhams, P.: Arctic ice cover, ice thickness and tipping points, AMBIO, Royal Swedish Acad. Sci., 41, 1, 23-33, 2012.

Wadhams, P., Hughes, N., and Rodrigues, J.: Arctic sea ice thickness characteristics in winter 2004 and 2007 from submarine sonar transects, J. Geophys. Res., 116, C00E02, doi:10.1029/2011JC006982, 2011.

Wadhams, P., Tucker III, W. B., Krabill, W. B., Swift, R. N., Comiso, J. C., and Davis, N. R.: Relationship between sea ice freeboard and draft in the Arctic Basin, and implications for ice thickness monitoring, J. Geophys. Res., 97(C12), 20,325–20,334, doi: 10.1029/92JC02014, 1992.

Warren, S. G., Rigor, I. G., Untersteiner, N., Radionov, V. F., Bryazgin, N. N., Aleksandrov, Y. I., and Colony, R.: Snow depth on Arctic sea ice, J. Clim., 12, 1814-1829, 1999.

Worby, A. P., Markus, T., Steer, A. D., Lytle, V. I., and Massom, R. A.: Evaluation of AMSR-E snow depth product over East Antarctic sea ice using in situ measurements and aerial photography, J. Geophys. Res., 113, C05S94, doi:10.1029/2007JC004181, 2008.

Yu, Y. and Rothrock, D. A.: Thin ice thickness from satellite thermal imagery, J. Geophys. Res., 101(C10), 25,753-25,766, 1996.

Zhang, J., Lindsay, R., Schweiger, A., and Rigor, I. G.: Recent changes in the dynamic properties of declining Arctic sea ice: A model study, Geophys. Res. Lett., 39, L20503, doi:10.1029/2012GL053545, 2012.

1 Table 1. Validation data used in the RRDP for sea ice thickness.

Year	Location	Parameter	Source	Acronym
2003-08	Beaufort Sea	Ice draft, snow depth	BGEP moored ULS, AMSR-E	BGEP
Apr 1994 Oct 1996	Beaufort Sea	Ice draft	NSIDC U.S. submarine ULS	BS
Mar 2007	Fram Strait, Beaufort Sea	Ice draft, snow depth	UCAM UK submarine ULS, AMSR-E	BSS
May 2011 Apr 2008	Fram Strait	Ice freeboard, thickness, snow depth	DTU ALS, ASIRAS, AMSR-E	FS
2009/10	Western Arctic	Ice freeboard, thickness, snow depth	NSIDC IceBridge	OIB

2

Table 2: Summary of the comparison between OIB, W99, and AMSR-E snow depth in the Arctic Ocean. Absolute values are only given for OIB; all other values are differences. All values are given together with one standard deviation.

Data set	All	MYI (> 65%)	FYI (> 95%)	Can. Arch.
OIB 2009	(0.26 ± 0.11) m	(0.36 ± 0.04) m	(0.16 ± 0.02) m	--
OIB – W99	(-0.07 ± 0.11) m	(0.02 ± 0.04) m	(-0.19 ± 0.02) m	--
OIB – AMSR-E	--	--	(-0.01 ± 0.02) m	--
W99 – AMSR-E	--	--	(0.18 ± 0.03) m	--
OIB 2010	(0.21 ± 0.07) m	(0.23 ± 0.05) m	(0.13 ± 0.02) m	(0.13 ± 0.04) m
OIB – W99	(-0.13 ± 0.07) m	(-0.12 ± 0.05) m	(-0.21 ± 0.01) m	--
OIB – AMSR-E	--	--	(-0.03 ± 0.02) m	(-0.01 ± 0.03) m
W99 – AMSR-E	--	--	(0.18 ± 0.02) m	--

Table 3: Summary of overall mean observed (OIB) and computed (RA-2) snow freeboard using OIB or W99 snow depth; given are mean values plus/minus one standard deviation.

Data set	Snow freeboard (OIB)	Snow freeboard (RA-2 + OIB snow depth)	Snow freeboard (RA-2 + W99 snow depth)
OIB 2009	(0.52 ± 0.15) m	(0.51 ± 0.10) m	(0.52 ± 0.07) m
OIB 2010	(0.42 ± 0.16) m	(0.40 ± 0.12) m	(0.53 ± 0.08) m

Table 4: Summary of observed and computed sea ice draft values using standard settings and W99 snow parameters; given are mean values plus/minus one standard deviation. See Table 1 for data set acronyms.

Data set	Observed draft (ULS)	Derived draft (RA, RA-2)
BS 1994	(2.92 ± 0.41) m	(2.47 ± 0.57) m
BS 1996	(1.68 ± 0.51) m	(1.81 ± 0.41) m
BSS 2007	(2.48 ± 0.46) m	(2.36 ± 0.54) m
BGEP 2003-2008	(1.59 ± 0.42) m	(1.64 ± 0.25) m

Table 5: Summary of comparison between RA-2 sea ice thickness computed using different snow depth data sets and OIB sea ice thickness for the Arctic Ocean. Total number of data pairs is N=43 for 2009 and N=90 for 2010.

Year	Snow data set	R	RMSD [m]	Year	Snow data set	R	RMSD [m]
2009	OIB	0.65	0.96	2010	OIB	0.38	1.52
	W99	0.57	1.00		W99	0.23	1.35
	AMSR-E + W99	0.62	1.02		AMSR-E + W99	0.34	1.41
	KF11	0.62	1.02		KF11	0.34	1.40

Table 6: Summary of comparison between RA-2 sea ice thickness computed using different snow depth data sets and OIB sea ice thickness for the Fram Strait area. Total number of data pairs is N=13.

Year	Snow data set	R	RMSE [m]
2010	W99	0.80	0.88
	OIB	0.84	1.03

Table 7: Differences of mean and median observed minus computed sea ice draft from submarine and moored ULS (see Table 1) and algorithms A1 to A6 applied to radar altimeter data for the Arctic Ocean. Algorithms giving the smallest difference are highlighted in bold font.

	Data set	A1	A2	A3	A4	A5	A6
Difference in mean (median) SID [m]	BS, 10/1996	0.13 (**0.03**)	-0.12 (-0.23)	0.06 (0.04)	0.13 (**0.03**)	0.49 (0.35)	**0.01** (-0.13)
	BGEP, 2002/03 – 2007/08	**-0.01** (**0.05**)	-0.22 (-0.19)	0.02 (0.09)	-0.04 (**0.05**)	0.16 (0.27)	-0.43 (-0.35)
	BSS, 03/2007	**0.00** (**0.01**)	-0.22 (-0.24)	0.08 (-0.15)	-0.36 (-0.33)	-0.46 (-0.40)	-0.69 (-0.70)

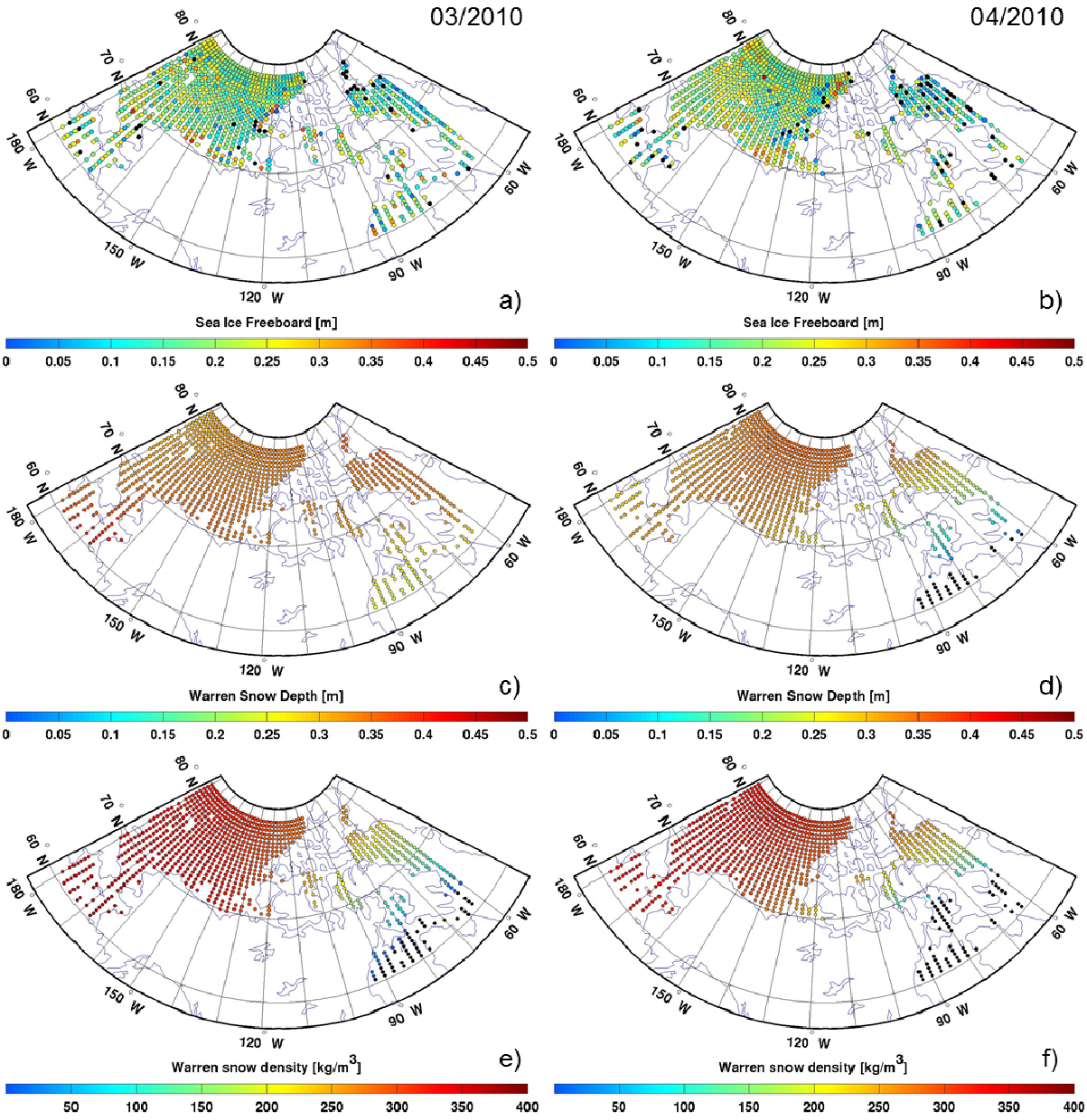

Figure 1: Maps of the collocated Envisat RA-2 sea ice freeboard for March and April 2010 (a, b), of the Warren Climatology snow depth (c, d) and of the Warren Climatology snow density (e, f). Negative values are flagged black.

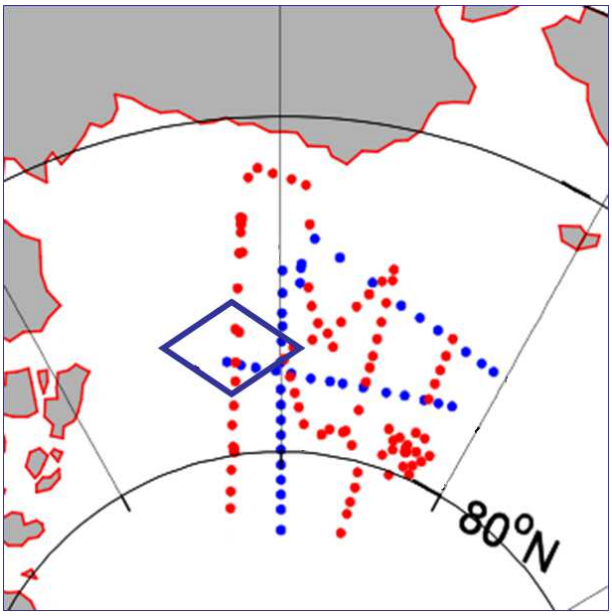

Figure 2: Location of U.S. submarine ULS draft measurements in blue (1994) and red (1996) together with the approximate location of the BGEP moorings (diamond).

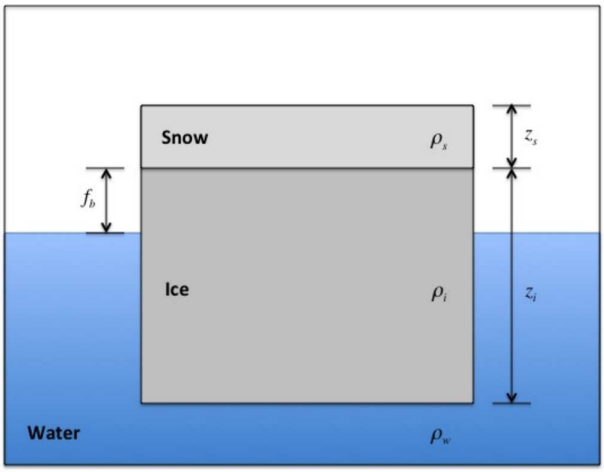

Figure 3: Illustration of the parameters involved in sea ice thickness computation using sea ice freeboard.

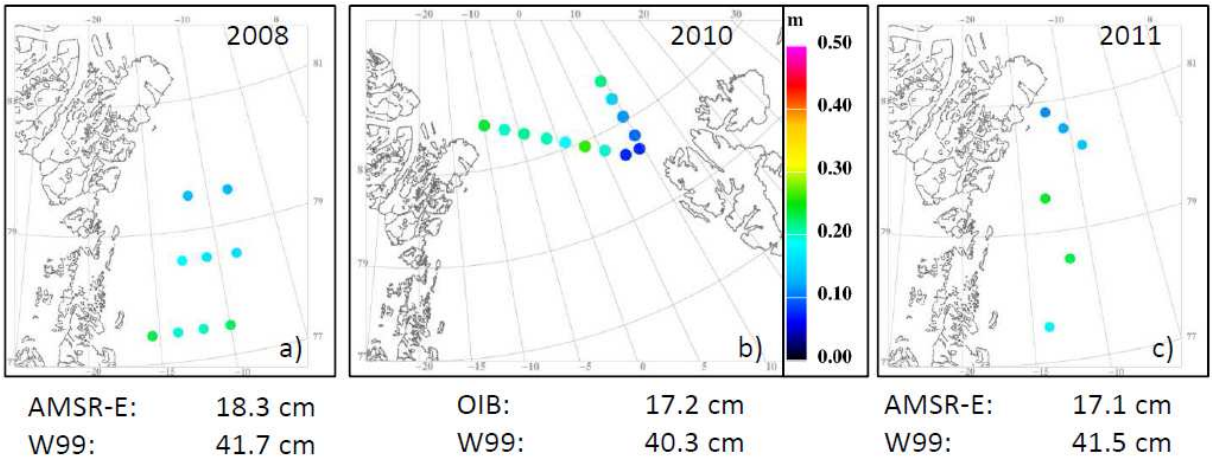

Figure 4: Locations and values for snow depth data sets in the Fram Strait for CryoVEx (a, c) and OIB (b). For CryoVEx only AMSR-E snow depths are shown as these are only available for FYI; for 2008 this is 9 out of 11 and for 2011 this is 6 out of 21 data points. In 2010 no FYI was present according to AMSR-E ice classification.

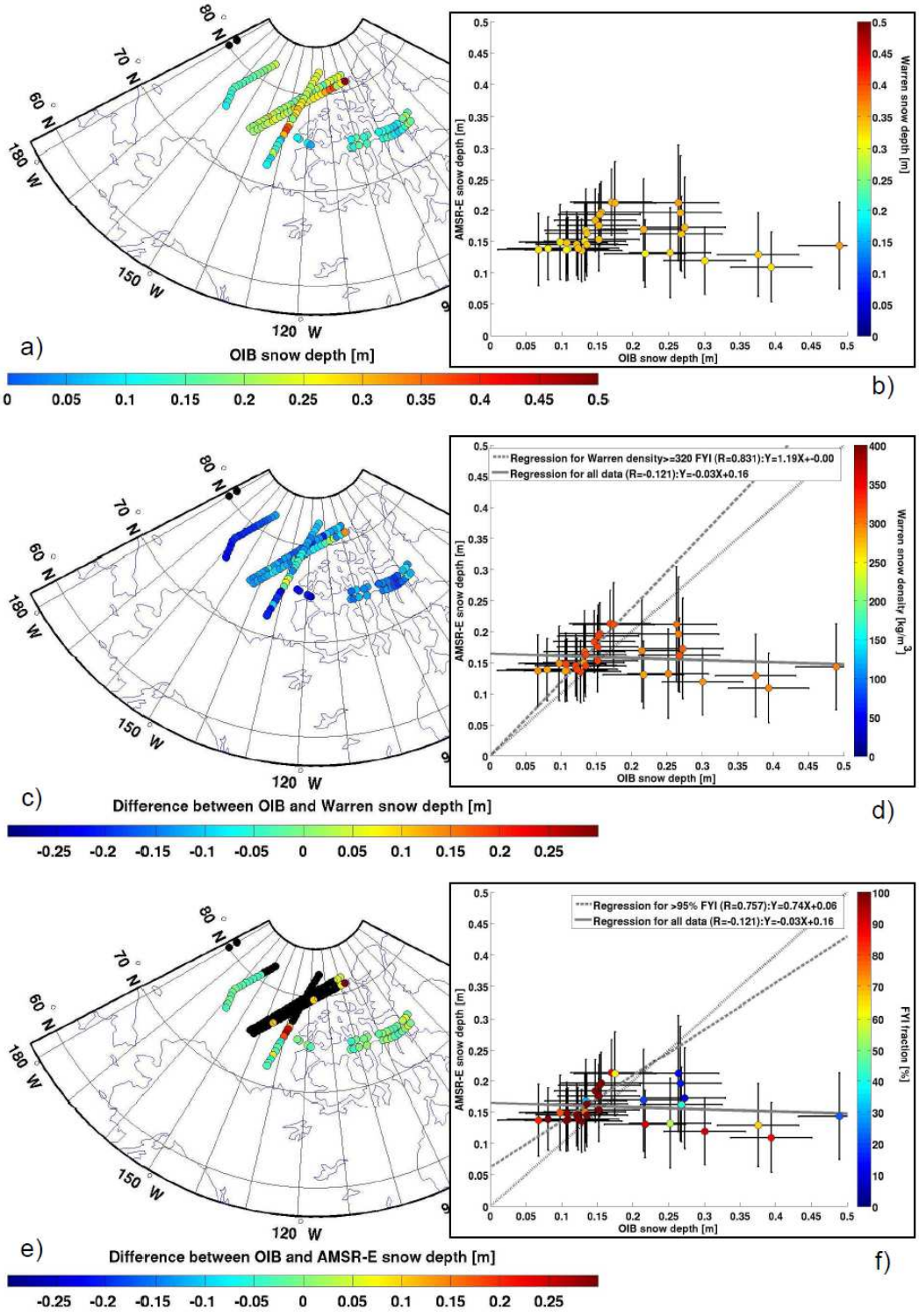

Figure 5: Left column: OIB snow depth and its difference to W99 and AMSR-E snow depth for April 2010. Grid cells with FYI fraction of 0% are flagged black in image e). Right column: Scatter plots of AMSR-E vs. OIB snow depth with symbols color coded with W99 snow depth (image b), W99 snow density (image d), and FYI fraction (image f). The grey solid line represents the 1-to-1 relationship; black solid and dashed lines are the regression

lines using all data pairs or in limitation to the given density (image d) and FYI fraction (image f) values. Note that the parallel tracks visible in images a), c) and e) are actually on top of each other. They have been separated by 0.4 degree latitude for better visibility.

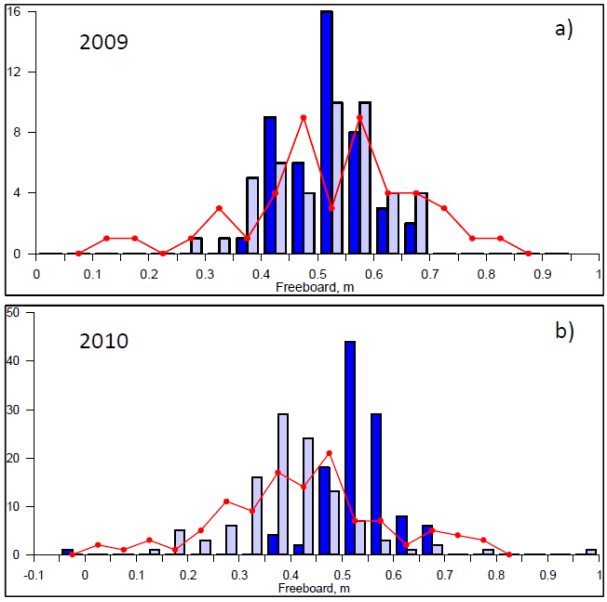

Figure 6: Histograms of OIB (red lines) and RA-2 (blue bars) freeboard. RA-2 freeboard is derived using OIB snow depth (light blue bars) and W99 snow depth (dark blue bars). Both MYI and FYI data are included. Note the different y-axis scaling.

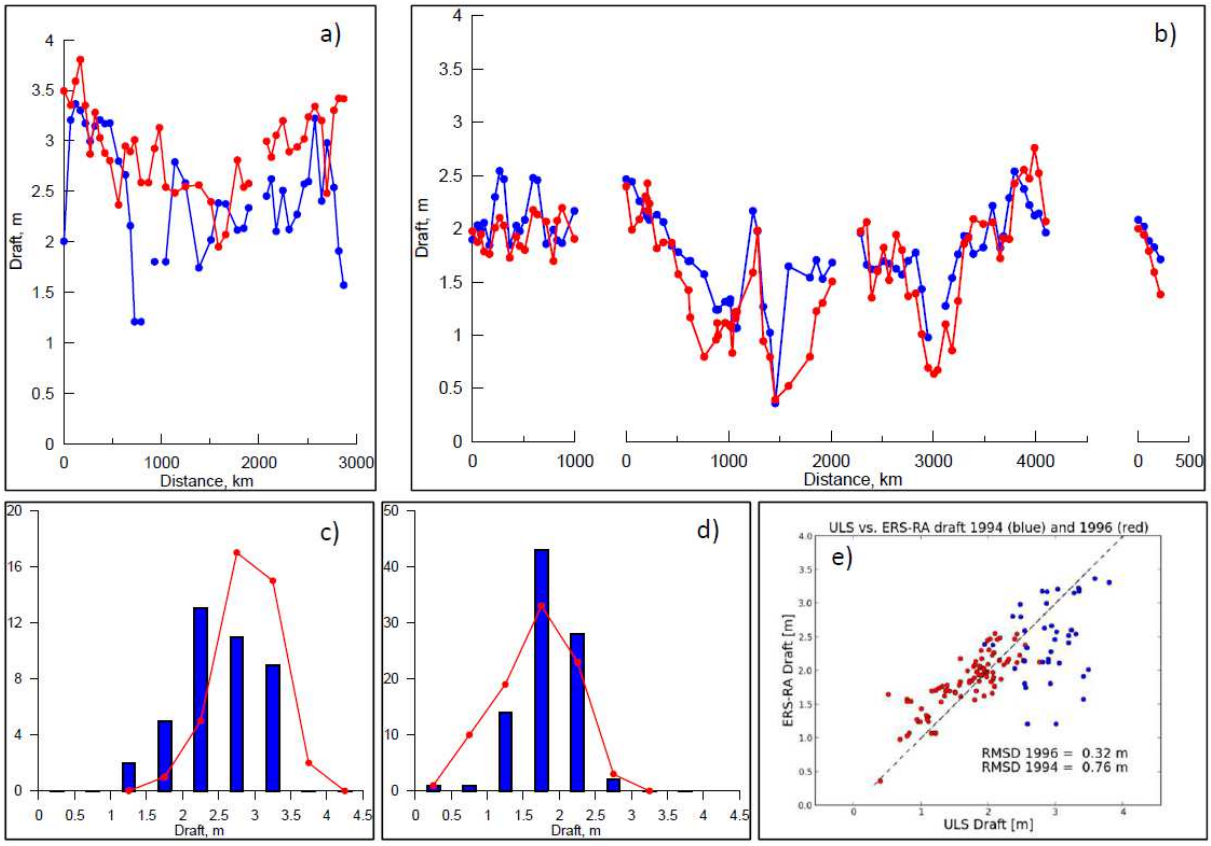

Figure 7: Comparison between sea ice draft observed from U.S. submarine ULS (red) and computed from ERS-1 RA sea ice freeboard using W99 snow data (blue). Images a) and b) are profiles along submarine track for April 1994 and October 1996, respectively (see also Figure 2); Images c) and d) show corresponding histograms. Image e) compares data from both cruises for 1994 (blue) and 1996 (red) together with the RMSD.

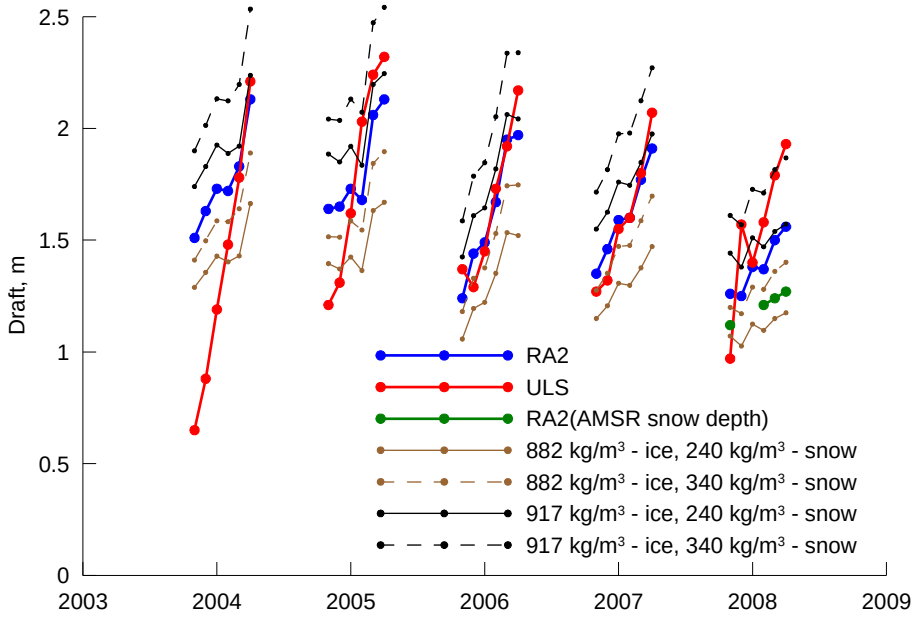

Figure 8: BGEP ULS draft data, averaged to monthly mean for the winter months October to March (red) compared to monthly mean draft computed from RA-2 sea ice freeboard using a) W99 snow depth and density and standard values: ρ_i = 900 kg m^{-3} and ρ_w = 1030 kg m^{-3} (blue); b) W99 snow depth but MYI density: ρ_i = 882 kg m^{-3} (brown); c) W99 snow depth and FYI density: ρ_i = 917 kg m^{-3} (black); and d) AMSR-E snow depth (green). Note that the latter is only possible for FYI areas. For b) and c) snow density is set fixed to either 240 kg m^{-3} (solid lines) or 340 kg m^{-3} (broken lines).

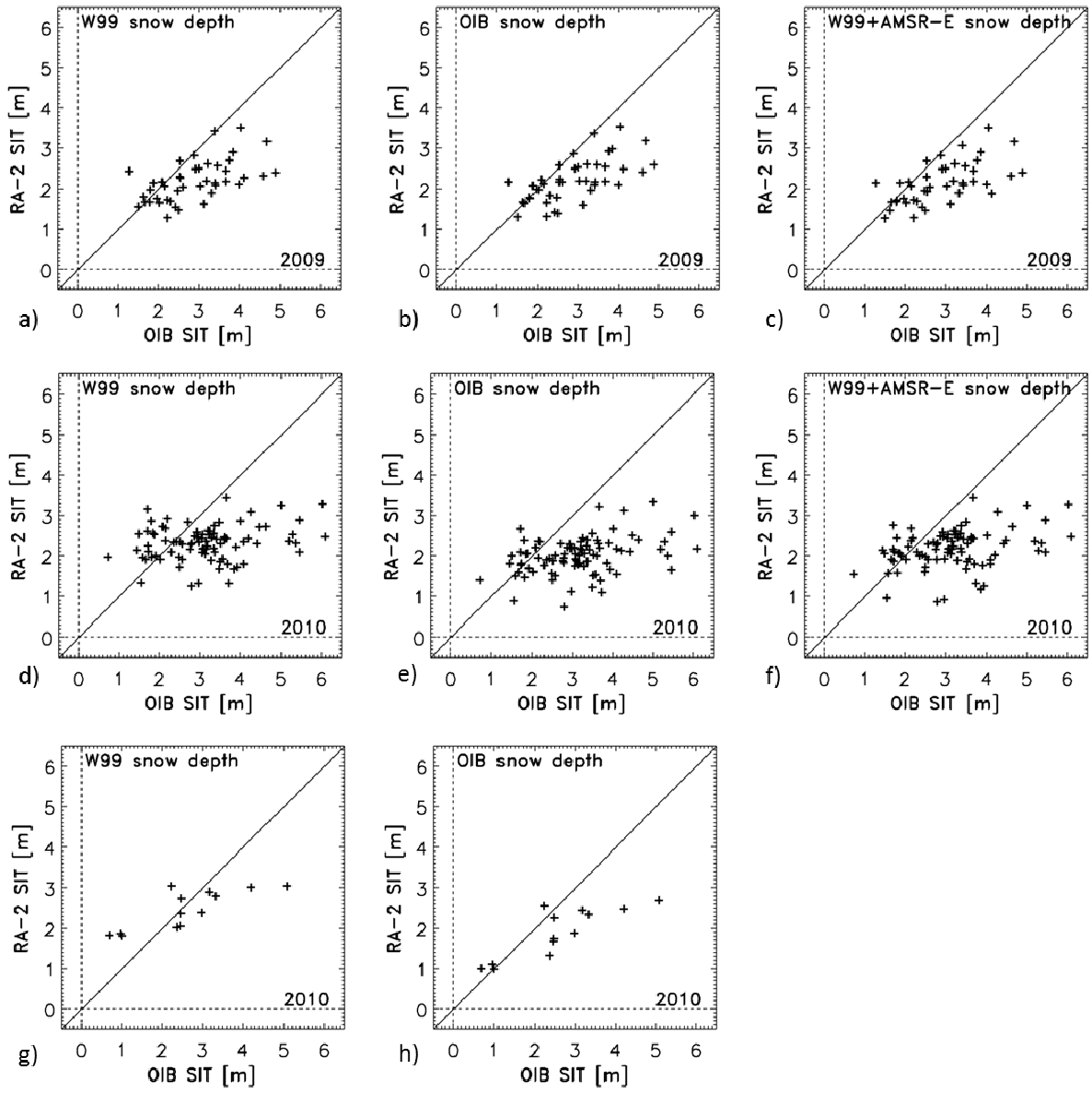

Figure 9: RA-2 sea ice thickness computed using different snow depth data sets versus OIB sea ice thickness for 2009 (a to c) and 2010 (d to h). Images a) to f) are for the Arctic Ocean, images g) and h) are for the Fram Strait area.